Why many Batesian mimics are inaccurate – Taylor, Reader and Gilbert 2016

Supporting information:

Supplementary methods – details of image processing (p. 1)

Supplementary results and discussion – rare model species (p. 3)

Figures S1-S5 (p. 4)

Tables S1-S7 (p. 9)

Table S8 is included as a separate file, and contains raw data for each individual insect

Supplementary methods – details of image processing

Image processing was carried out in MATLAB [1]. Three landmarks were selected by eye on each image (Figure S2A): 1, the tip of the abdomen, and 2 and 3, points at either side of the top of the abdomen. In hoverflies, 2 and 3 were located where the sides of abdominal tergite 2 met the scutellum, whilst in wasps, they were where the first tergite met the petiole. A further point, 4, was defined as the midpoint between 2 and 3, and the image rotated so that the line of symmetry running from 1 to 4 was vertical (with point 1 at the base). The image was also rescaled to fix the length of the abdomen at 100 pixels, and a smoothing algorithm was applied ["rotating mask"; 2] – see Figure S2B.

An edge detection algorithm then searched for an outline that joined 1 to 2 and 3, respectively (Figure S2C). In about half of all cases, this algorithm was effective in finding the outline of the abdomen (as checked by eye), but sometimes failed when “distracted” by other features in the image with a strong outline, such as legs lying close to the abdomen. In these latter cases, a “guide line” was drawn by eye, and then the algorithm was re-run, restricted to searching within 3 pixels of the guide (Figure S2D). This compromise between automated and user-driven processing allowed manual processing time and subjective input to be kept to a minimum whilst ensuring the effective separation of abdomen from background. The resulting outline, completed by a horizontal line across from the lower of points 2 and 3, defined the region of interest on which subsequent calculations were carried out.

The abdomen was segmented into two colour regions (typically black and yellow/orange; Figure S2E) using two alternative methods. For the first, the image was converted to greyscale by calculating the first principal component of the R, G and B values for all pixels. This resulted in a greyscale image in which the variation in brightness was maximised. This image was then segmented using a cut-off threshold calculated from Otsu’s method [3]. In the second method, for each pixel, the lowest of its three colour values (R, G or B) was subtracted from all three colour channels for that pixel, essentially giving its variation from grey, or saturation. The image was then converted to greyscale using principal components and segmented as in the first method.

Due to variation in colour among individual insects, as well as slight changes in lighting conditions among photographs, these two methods varied in their effectiveness at capturing the binary abdominal pattern. We therefore segmented each image using both methods and chose, by eye, the resulting segmentation that most closely represented the pattern as seen in the original image. Note that in many cases both methods produced a highly accurate segmentation and had only subtle differences. Some images (129 out of 968) did not produce good segmentations using either method and were discarded from further analyses.

To quantify the colour proportions in the pattern, we calculated the proportion of pixels within the abdominal image that were classified as “black” (i.e. the darker of the two segments) after segmentation.

[1] MATLAB. 2012 MATLAB. (Natick, Massachusetts, The Mathworks.
[2] Sonka, M., Hlavac, V. & Boyle, R. 2008 *Image Processing, Analysis, and Machine Vision*. Third ed, Thomson.
[3] Otsu, N. 1975 A threshold selection method from gray-level histograms. *Automatica* **11**, 285-296.

Supplementary results and discussion - rare model species

In addition to the four main model species analysed in the main text, we found eight further species of yellow-and-black Hymenoptera in our samples in small numbers: *Ancistrocerus trifasciatus* (N = 3), *Ectemnius cavifrons* (3), *Dolichovespula saxonica* (2), *Mellinus arvensis* (2), *Crossocerus binotatus* (1), *Ectemnius continuus* (1), *Nomada goodeniana* (1) and *Nomada marshamella* (1). We excluded these from the main analysis on the basis that they are unlikely to have much of an effect on predator learning in these communities due to their scarcity. However, it is possible that population sizes may have been different in the past, and therefore there is still the potential that they could have shaped the evolution of the mimics within the community.

Here we briefly present a parallel analysis to that presented in the main body of the paper (four models, or 4M), repeated using all twelve possible model species (12M).

1. Relaxed selection

As with the 4M analysis, none of the included predictors had a significant effect on pattern variability (Table S4).

2. Multiple models

Repeating this analysis with 12M rather than 4M greatly increases its complexity: rather than looking at six possible pairings of model species, we now have 66. There are 34 different SSUs for which we have data for six or more individuals, giving a total of 2244 tests of correlation. The scope for false positives is therefore high; even if none of the species have a true negative correlation, we would expect to detect a significant negative correlation in approximately 56 cases (2.5% of the total) if each test were independent.

In reality, we find only 30 examples of negative correlations, spread amongst 14 different mimic species. We can expect that at least the majority of these will be false positives. Even if a small scattering of genuine negative correlations do exist, which could indicate potential trade-offs in a few species, it appears that the community as a whole is not being shaped by these trade-offs.

3. Thermoregulation

This repeat analysis yields a similar set of predictors for mimetic accuracy, although the interaction between sex and season is no longer significant, while there is an interaction between proportion black and season (Table S6). Changes in the coefficients, once the interactions are taken into account, reflect a weaker effect of proportion black on accuracy. In this analysis, only the large males show a clear decrease in mimetic accuracy with increasing black in the pattern (Figure S5).

Supplementary Figures

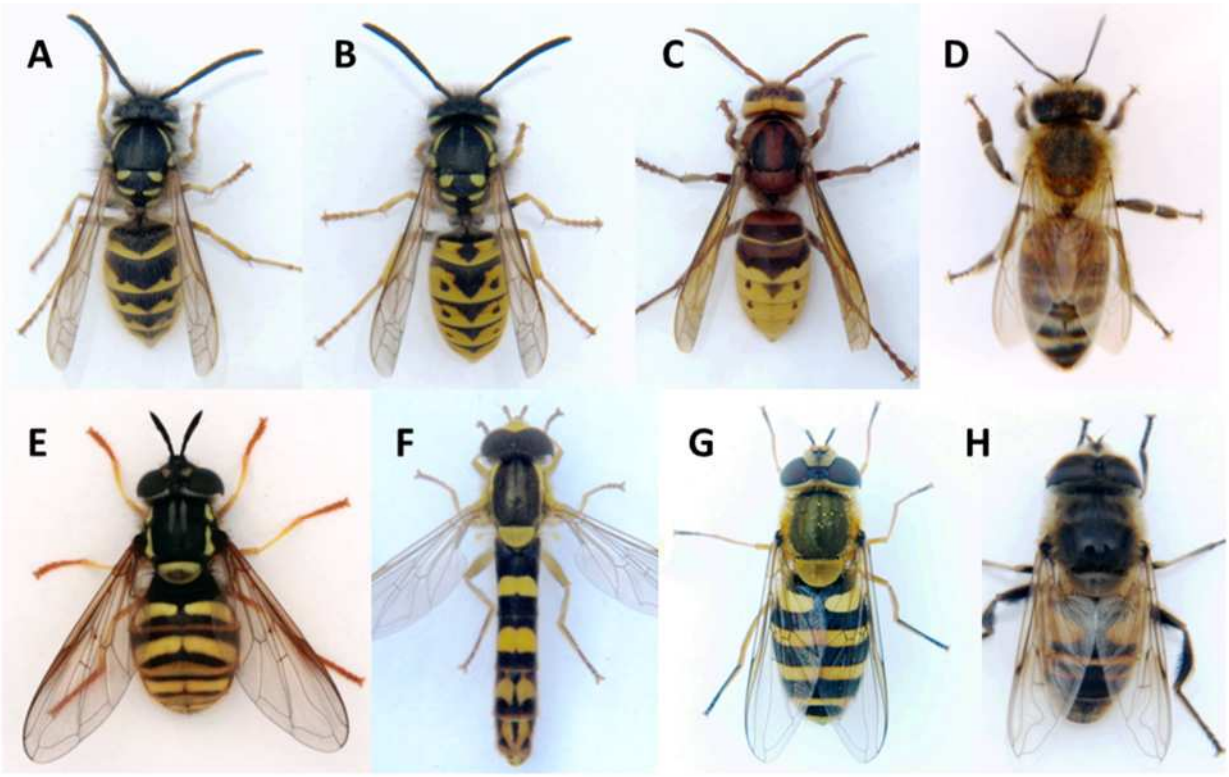

Figure S1. Photographs of live specimens of a selection of species that feature in this study. Hymenoptera: A *Vespula vulgaris*; B *Vespula germanica*; C *Vespa crabro*; D *Apis mellifera*. Syrphidae: E *Chrysotoxum arcuatum*; F *Sphaerophoria scripta*; G *Syrphus ribesii*; H *Eristalis tenax*.

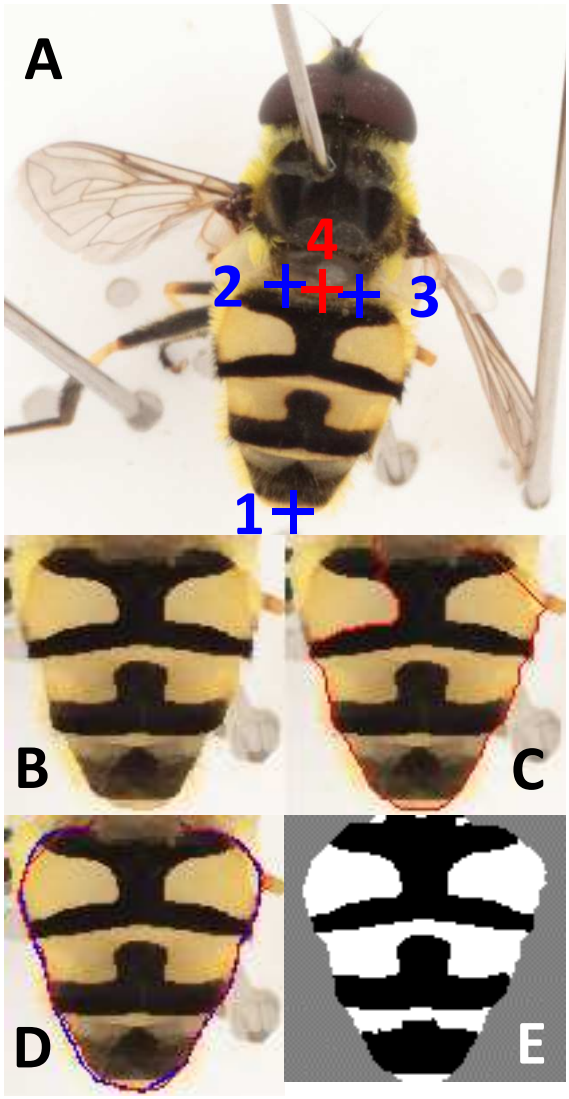

Figure S2. Image processing example (*Myathropa florea*). All steps were automated except those shown in blue. A: The user selects three control points on the image to identify the abdomen. A fourth point is calculated automatically as midway between 2 and 3. B: The image is scaled to a height of 100 pixels, cropped, rotated and smoothed. C: An edge detection algorithm is used to connect point 1 to 2 and 3. D: When necessary, the user draws a rough outline (blue) which is used to "guide" the edge detection algorithm to a more appropriate result (red). E: RGB pixel values are used to split the abdomen image into two "segments", one for yellow and one for black.

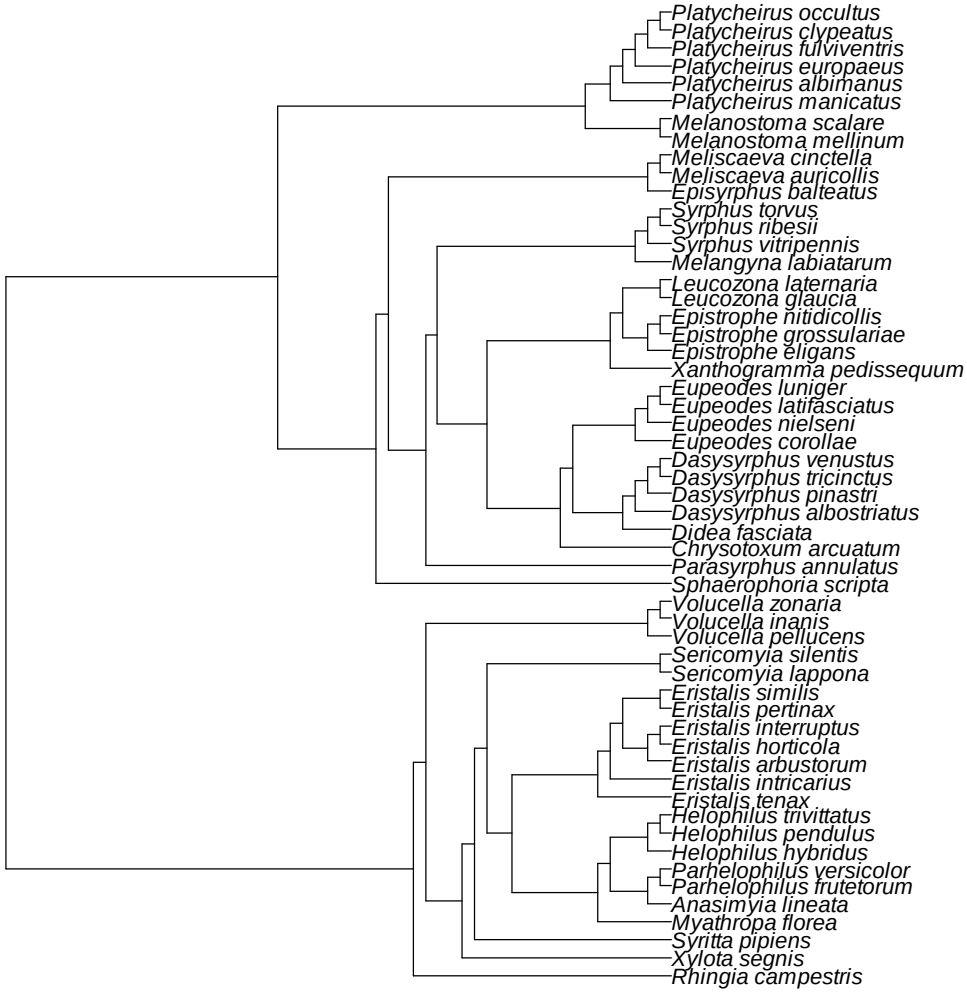

Figure S3. Phylogeny of the Syrphid species appearing in our samples. Used to control for relatedness among species in our analyses. This tree was assembled using data both morphological and molecular data (51 and 52). Branch lengths were assigned using Grafen's method (47).

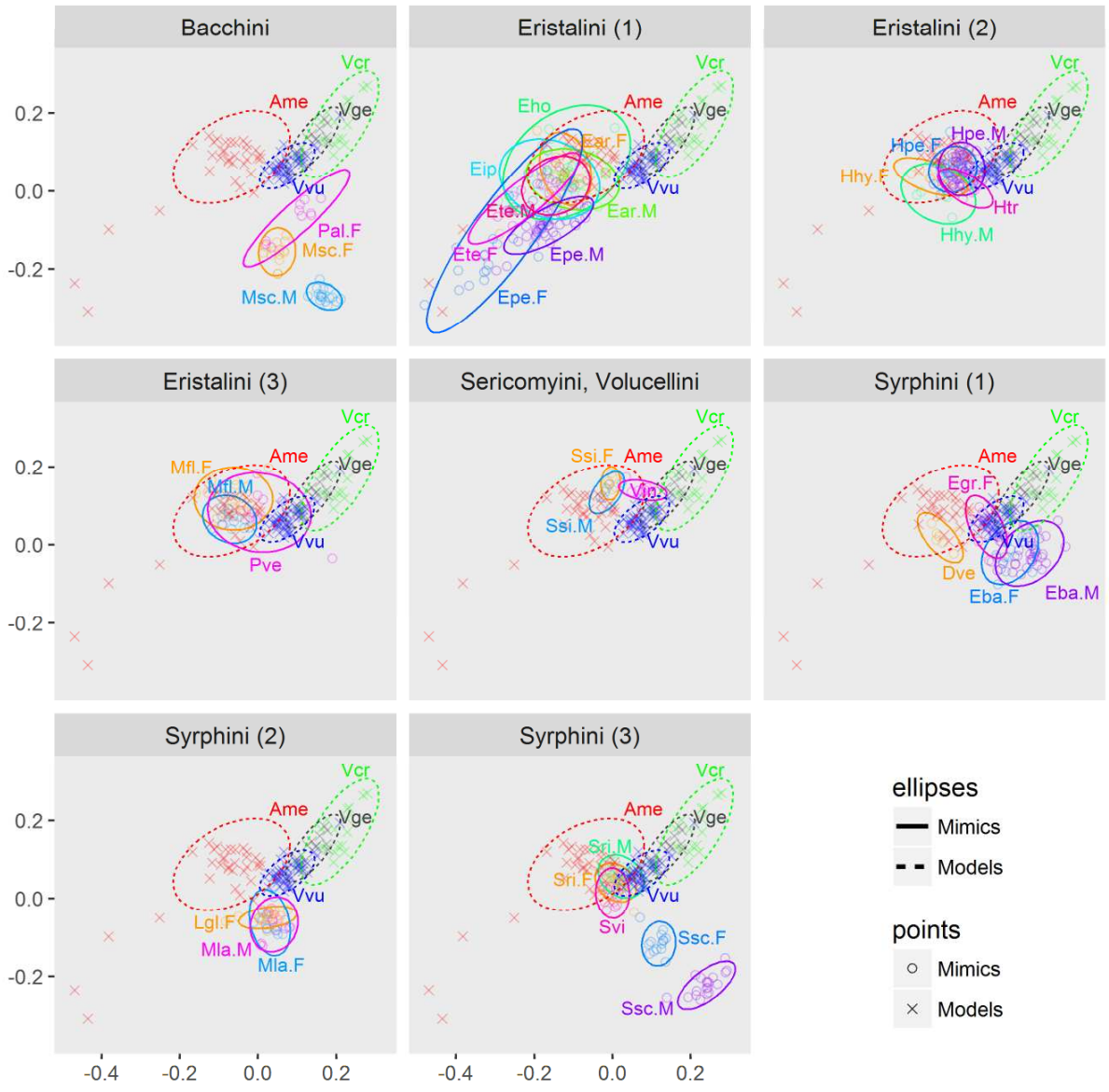

Figure S4. Models and mimics plotted in similarity space using the first two dimensions from CMDS. SSUs with N < 6 are not plotted. Ellipses show 95% confidence limits for each SSU, calculated from a modelled multivariate normal distribution based on the individual data points. SSUs are divided amongst panels according to their tribes and genera for clarity. See Table S2 for abbreviations.

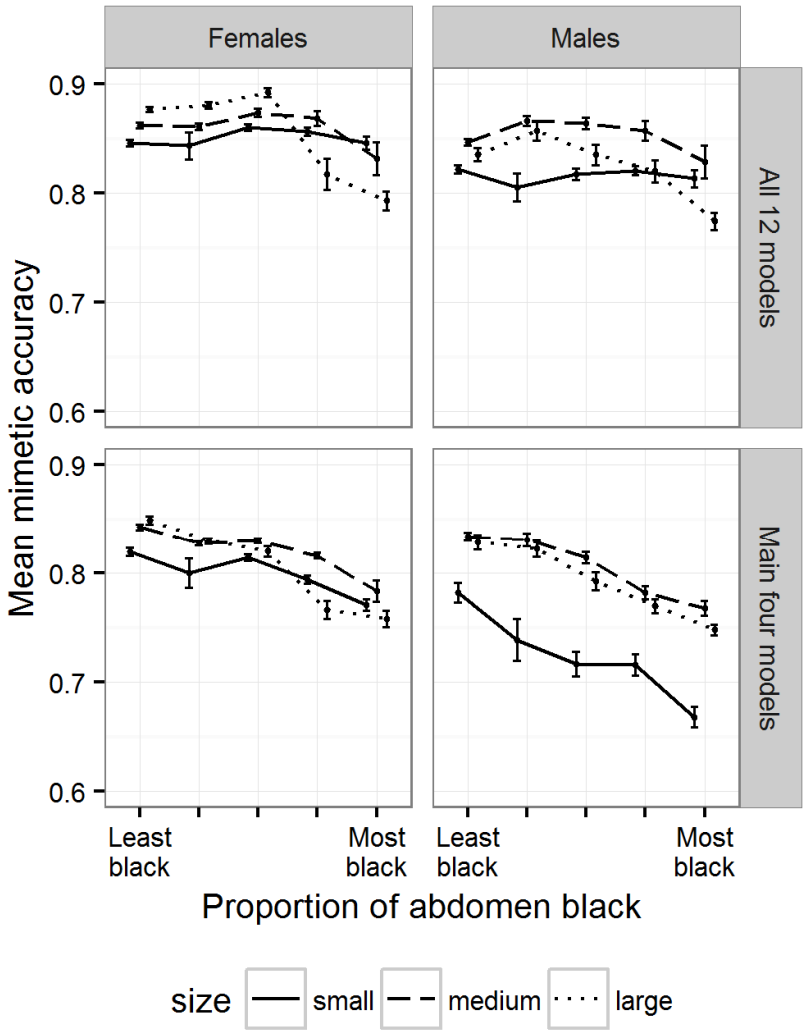

Figure S5. The effect of colour ratio on mimetic accuracy. Accuracy is calculated separately based on both all 12 models (top row) and the main four models (bottom row). Hoverfly individuals have been binned into three size categories in equal proportions: small (thorax up to 2.5mm wide; red), medium (2.6 to 3.8mm; green) and large (3.9mm or more; blue), and five colour categories (up to 52% black, 53-59% black, 60-66% black, 67-74% black, and 75% or more black). Error bars show ± standard error.

Supplementary Tables

Table S1. Brief descriptions of sampling sites used in this study. Note that totals are only for individuals that were included in the analysis – specimens for which images did not segment well are excluded.

Name	Latitude	Longitude	Description	Number of individuals
Attenborough Nature Reserve	52.91	-1.22	Wetland, former gravel pits	394
Cromford Canal	53.1	-1.53	Canal through deciduous woodland	131
Upper Moor	53.18	-1.54	Coniferous plantation	109
Grace Dieu Wood	52.76	-1.36	Deciduous woodland	84
Wollaton	52.96	-1.22	Allotment	30
University Lake	52.93	-1.2	Lakeside scrub	19
Piper Wood	52.79	-1.3	Deciduous woodland	17
Treswell Wood	53.31	-0.86	Deciduous woodland	12
Belton	52.78	-1.34	Rural garden	6
Shirland	53.12	-1.41	Rural garden	5
Dovedale Wood	53.07	-1.79	Deciduous woodland	5
Dovedale House	53.05	-1.8	Pasture	3
Harrow Road	52.95	-1.21	Suburban garden	3
Staunton Harold Reservoir	52.81	-1.44	Lakeside scrub	2
Calke Abbey	52.8	-1.46	Rural garden	2
Swineholes Wood	53.05	-1.93	Scrub/moorland	2
Monsal Dale	53.24	-1.71	Pasture	1

Table S2. Results for tests of sexual dimorphism, for those species with N ≥ 3 for both sexes. Size was tested using Wilcoxon two-sample test, and pattern was tested using distance-based ANOVA with a permutation test. Significant p values are highlighted in bold. * Numbers in brackets refer to N for size measurements.

Species	N* female	N* male	Size test: W	Size test: p	Pattern test: pseudo-F	Pattern test: p
Epistrophe grossulariae	16	3	38.5	0.112	10.45	**0.0009**
Episyrphus balteatus	17	37	106.5	**0.0001**	7.56	**0.0002**
Eristalis arbustorum	17 (16)	26	291.5	**0.030**	44.38	**0.0001**
Eristalis pertinax	26 (22)	47 (45)	332.5	**0.030**	37.95	**0.0001**
Eristalis tenax	9	15	94.5	0.109	7.65	**0.012**
Helophilus hybridus	7	7 (6)	28	0.351	28.61	**0.0001**
Helophilus pendulus	35 (32)	54 (52)	1091	**0.017**	25.51	**0.0001**
Helophilus trivittatus	3 (2)	4	-	-	2.24	0.147
Leucozona glaucia	18	4	38.5	0.862	4.25	**0.018**
Melangyna labiatarum	12 (6)	16 (2)	-	-	4.47	**0.016**
Melanostoma scalare	15	17 (15)	81	0.185	119.4	**0.0001**
Myathropa florea	18 (14)	14 (13)	69.5	0.306	5.64	**0.002**
Parhelophilus versicolor	3 (2)	10 (9)	-	-	2.6	0.080
Platycheirus albimanus	10	4	1	**0.008**	2.26	0.144
Platycheirus fulviventris	3	4	5	0.852	8.74	**0.003**
Sericomyia silentis	7	7	10.5	0.080	10.93	**0.0003**
Sphaerophoria scripta	14	19	86	0.086	51.44	**0.0001**
Syritta pipiens	4	4	16	**0.028**	18.04	**0.003**
Syrphus ribesii	24 (22)	21	149.5	**0.047**	7.3	**0.0002**
Syrphus vitripennis	12 (11)	6	16.5	0.102	2.7	0.056
Volucella pellucens	4	4	7.5	1.000	35.97	**0.008**

Table S3. Descriptive data for the model and mimic species sampled. Males and females are treated separately for sexually dimorphic mimic species (see Methods in main text). Models which were not included in the main analysis due to small sample size are listed in square brackets. These were also discounted when assigning the model for each mimic SSU. * N in brackets is the number of individuals with size recorded, where this differs from the total.

Species or Sex Unit	Abbrev.	Type	N*	Thorax width (mm)	Model	Accuracy	Proportion of the pattern that is black
Anasimiya lineata	Ali	Mimic	1	2.7	Vvu	0.833	0.64
Anicstrocerus trifasciatus	Atr	[Model]	3	2.2	-	-	0.70
Apis mellifera	Ame	Model	33 (25)	3.6	-	-	0.62
Chrysotoxum arcuatum	Car	Mimic	2	2.7	Vcr	0.848	0.46
Crossocerus binotatus	Cbi	[Model]	1	2.2	-	-	0.53
Dasysyrphus albostriatus	Dal	Mimic	4 (3)	2.5	Vvu	0.799	0.71
Dasysyrphus pinastri	Dpi	Mimic	1	2.6	Vvu	0.786	0.83
Dasysyrphus tricinctus	Dtr	Mimic	2	2.5	Vvu	0.809	0.84
Dasysyrphus venustus	Dve	Mimic	7 (6)	2.4	Ame	0.807	0.79
Didea fasciata	Dfa	Mimic	1	3.0	Vvu	0.830	0.62
Dolichovespula saxonica	Dsa	[Model]	2	3.0	-	-	0.64
Ectemnius cavifrons	Eca	[Model]	3	3.0	-	-	0.59
Ectemnius continuus	Ect	[Model]	1	2.8	-	-	0.73
Epistrophe eligans	Eel	Mimic	2 (0)	-	Ame	0.736	0.83
Epistrophe grossulariae F	Egr.F	Mimic	16	3.1	Vvu	0.820	0.54
Epistrophe grossulariae M	Egr.M	Mimic	3	2.9	Vvu	0.782	0.46
Epistrophe nitidicollis	Ent	Mimic	1 (0)	-	Vvu	0.848	0.58
Episyrphus balteatus F	Eba.F	Mimic	17	2.2	Vvu	0.828	0.48
Episyrphus balteatus M	Eba.M	Mimic	37	2.5	Vge	0.802	0.47
Eristalis arbustorum F	Ear.F	Mimic	17 (16)	3.5	Ame	0.798	0.77
Eristalis arbustorum M	Ear.M	Mimic	26	3.3	Vvu	0.789	0.64
Eristalis horticola	Eho	Mimic	9	3.6	Ame	0.791	0.68
Eristalis interruptus	Eip	Mimic	7	3.5	Ame	0.784	0.76
Eristalis intricarius	Eic	Mimic	5	4.4	Vvu	0.778	0.54
Eristalis pertinax F	Epe.F	Mimic	26 (22)	3.7	Ame	0.732	0.79
Eristalis pertinax M	Epe.M	Mimic	47 (45)	3.9	Ame	0.749	0.74
Eristalis tenax F	Ete.F	Mimic	9	4.5	Ame	0.780	0.78
Eristalis tenax M	Ete.M	Mimic	15	4.4	Ame	0.780	0.66
Eupeodes corollae	Eco	Mimic	4 (3)	2.2	Vvu	0.839	0.60
Eupeodes latifasciatus	Ela	Mimic	1	2.0	Vvu	0.833	0.55
Eupeodes luniger	Elu	Mimic	2	2.7	Vvu	0.813	0.69
Eupeodes nielseni	Enl	Mimic	3 (0)	-	Vvu	0.796	0.76
Helophilus hybridus F	Hhy.F	Mimic	7	3.8	Vvu	0.810	0.64
Helophilus hybridus M	Hhy.M	Mimic	7 (6)	3.6	Vvu	0.752	0.54
Helophilus pendulus F	Hpe.F	Mimic	35 (32)	3.4	Vvu	0.844	0.56
Helophilus pendulus M	Hpe.M	Mimic	54 (52)	3.2	Vvu	0.844	0.53
Helophilus trivittatus	Htr	Mimic	7 (6)	4.1	Vvu	0.833	0.54

Leucozona glaucia F	Lgl.F	Mimic	18	2.7	Vvu	0.802	0.67
Leucozona glaucia M	Lgl.M	Mimic	4	2.8	Vvu	0.785	0.70
Leucozona laternaria	Lla	Mimic	2	2.5	Vvu	0.762	0.75
Melangyna labiatarum F	Mla.F	Mimic	12 (6)	1.9	Vvu	0.830	0.73
Melangyna labiatarum M	Mla.M	Mimic	16 (2)	2.1	Vvu	0.800	0.73
Melanostoma mellinum	Mme	Mimic	4	1.7	Vvu	0.706	0.68
Melanostoma scalare F	Msc.F	Mimic	15	1.6	Vvu	0.755	0.76
Melanostoma scalare M	Msc.M	Mimic	17 (15)	1.7	Vvu	0.638	0.74
Meliscaeva auricollis	Mau	Mimic	1	2.0	Vvu	0.778	0.67
Meliscaeva cinctella	Mci	Mimic	3 (2)	1.9	Vvu	0.782	0.56
Mellinus arvensis	Mar	[Model]	2	2.2	-	-	0.60
Myathropa florea F	Mfl.F	Mimic	18 (14)	3.6	Vvu	0.817	0.59
Myathropa florea M	Mfl.M	Mimic	14 (13)	3.7	Vvu	0.833	0.60
Nomada goodeniana	Ngo	[Model]	1	3.1	-	-	0.57
Nomada marshamella	Nma	[Model]	1	3.2	-	-	0.73
Parasyrphus annulatus	Pan	Mimic	2	2.4	Vvu	0.755	0.56
Parhelophilus frutetorum	Pfr	Mimic	4 (2)	3.0	Vvu	0.860	0.56
Parhelophilus versicolor	Pve	Mimic	13 (11)	3.1	Vvu	0.866	0.56
Platycheirus albimanus F	Pal.F	Mimic	10	1.7	Vvu	0.797	0.63
Platycheirus albimanus M	Pal.M	Mimic	4	2.0	Vvu	0.735	0.70
Platycheirus clypeatus	Pcl	Mimic	4 (3)	1.7	Vvu	0.766	0.68
Platycheirus europaeus	Peu	Mimic	1	1.7	Vvu	0.747	0.79
Platycheirus fulviventris F	Pfu.F	Mimic	3	1.7	Vvu	0.778	0.46
Platycheirus fulviventris M	Pfu.M	Mimic	4	1.7	Vge	0.703	0.46
Platycheirus manicatus	Pma	Mimic	2	1.9	Vvu	0.774	0.67
Platycheirus occultus	Poc	Mimic	1	1.5	Vvu	0.756	0.74
Rhingia campestris	Rca	Mimic	3	2.5	Vcr	0.803	0.33
Sericomyia lappona	Sla	Mimic	3	3.7	Vcr	0.791	0.82
Sericomyia silentis F	Ssi.F	Mimic	7	4.3	Vcr	0.807	0.69
Sericomyia silentis M	Ssi.M	Mimic	7	4.6	Vcr	0.813	0.69
Sphaerophoria scripta F	Ssc.F	Mimic	14	1.6	Vvu	0.777	0.68
Sphaerophoria scripta M	Ssc.M	Mimic	19	1.7	Vvu	0.645	0.61
Syritta pipiens F	Spi.F	Mimic	4	2.1	Vvu	0.757	0.81
Syritta pipiens M	Spi.M	Mimic	4	1.7	Vvu	0.638	0.80
Syrphus ribesii F	Sri.F	Mimic	24 (22)	2.8	Vvu	0.830	0.62
Syrphus ribesii M	Sri.M	Mimic	21	2.9	Vvu	0.826	0.59
Syrphus torvus	Sto	Mimic	4	2.9	Vvu	0.828	0.62
Syrphus vitripennis	Svi	Mimic	18 (17)	2.4	Vvu	0.818	0.64
Vespa crabro	Vcr	Model	18 (17)	5.6	-	-	0.48
Vespula germanica	Vge	Model	14 (11)	3.4	-	-	0.40
Vespula vulgaris	Vvu	Model	47 (41)	3.0	-	-	0.51
Volucella inanis	Vin	Mimic	7	4.8	Vge	0.811	0.35
Volucella pellucens F	Vpe.F	Mimic	4	4.9	Ame	0.667	0.68
Volucella pellucens M	Vpe.M	Mimic	4	4.9	Ame	0.668	0.70
Volucella zonaria	Vzo	Mimic	2	6.1	Vcr	0.820	0.59
Xanthogramma pedissequum	Xpe	Mimic	1	2.5	Vvu	0.815	0.76

Xylota segnis	Xse	Mimic	4	2.6	Vcr	0.551	0.56

Table S4. Results of GLS analysis of pattern variability, with predictors accuracy, size and their interaction. Results are displayed for analysis that included all twelve model species as well as those for just the main four models.

		Main four models only		All model species	
sex	predictor	Likelihood ratio	p	Likelihood ratio	p
Females (N = 32)					
	accuracy:size	0.1	0.748	2.64	0.104
	accuracy	0.82	0.365	0.87	0.35
	size	1.09	0.296	0.43	0.512
Males (N = 34)					
	accuracy:size	0.63	0.427	0.08	0.78
	accuracy	0.87	0.35	1.66	0.197
	size	0.73	0.392	0.42	0.517

Table S5. Correlation (Pearson's r) within each SSU (with N ≥ 6) among similarity values to each of the four main model species. Significant correlations at $p < 0.05$ are highlighted in bold. Note that all but one of the significant correlations are positive.

SSU	N	*V. vulgaris* - *V.germanica*	*V. vulgaris* - *V.crabro*	*V. germanica* - *V. crabro*	*V. vulgaris* - *A. mellifera*	*V. germanica* - *A. mellifera*	*V. crabro* - *A. mellifera*
Dasysyrphus venustus	7	**0.96**	0.75	**0.76**	0.14	0.33	-0.02
Eristalis arbustorum F	17	**0.98**	**0.93**	**0.96**	**0.62**	**0.67**	**0.65**
Eristalis arbustorum M	26	**0.99**	**0.93**	**0.94**	0.19	0.15	0.00
Episyrphus balteatus F	17	**0.94**	**0.84**	**0.76**	**0.69**	**0.64**	0.31
Episyrphus balteatus M	37	**0.89**	**0.62**	**0.59**	**0.68**	**0.48**	0.04
Epistrophe grossulariae F	16	**0.89**	**0.62**	**0.72**	0.10	0.10	0.10
Eristalis horticola	9	**0.98**	**0.95**	**0.96**	**0.68**	**0.68**	0.54
Eristalis interruptus	7	**0.99**	**0.96**	**0.97**	0.72	**0.77**	0.69
Eristalis pertinax F	26	**1.00**	**0.98**	**0.99**	**0.91**	**0.92**	**0.86**
Eristalis pertinax M	47	**1.00**	**0.95**	**0.97**	**0.90**	**0.90**	**0.83**
Eristalis tenax F	9	**0.99**	**0.98**	**0.99**	**0.76**	**0.80**	**0.77**
Eristalis tenax M	15	**0.99**	**0.85**	**0.89**	0.35	0.29	-0.11
Helophilus hybridus F	7	**0.98**	**0.95**	**0.93**	0.74	**0.80**	**0.77**
Helophilus hybridus M	7	**0.95**	**0.81**	**0.93**	0.39	0.17	0.07
Helophilus pendulus F	35	**0.92**	**0.79**	**0.76**	0.00	-0.11	-0.10
Helophilus pendulus M	54	**0.93**	**0.72**	**0.79**	0.14	0.02	-0.11
Helophilus trivittatus	7	**0.91**	**0.82**	**0.84**	-0.10	-0.39	-0.12
Leucozona glaucia F	18	**0.97**	**0.85**	**0.82**	-0.27	-0.35	-0.30
Myathropa florea F	18	**0.97**	**0.82**	**0.88**	**0.57**	**0.54**	0.15
Myathropa florea M	14	**0.97**	**0.81**	**0.81**	-0.02	0.14	-0.22
Melangyna labiatarum F	12	**0.97**	**0.90**	**0.90**	0.26	0.37	0.30
Melangyna labiatarum M	16	**0.99**	**0.92**	**0.92**	0.45	0.44	0.35
Melanostoma scalare F	15	**0.99**	**0.91**	**0.90**	**0.74**	**0.71**	**0.73**
Melanostoma scalare M	17	**0.98**	**0.90**	**0.91**	**0.93**	**0.88**	**0.73**
Platycheirus albimanus F	10	**0.99**	**0.91**	**0.89**	0.00	-0.11	-0.05
Parhelophilus versicolor	13	**0.87**	**0.70**	**0.79**	0.16	-0.14	-0.27
Syrphus ribesii F	24	**0.89**	**0.91**	**0.85**	-0.07	0.01	-0.26
Syrphus ribesii M	21	**0.82**	**0.75**	**0.44**	-0.25	0.05	**-0.56**
Sphaerophoria scripta F	14	**0.98**	**0.90**	**0.88**	**0.79**	**0.73**	**0.77**
Sphaerophoria scripta M	19	**0.76**	**0.72**	**0.89**	0.45	0.00	0.05
Sericomyia silentis F	7	**0.89**	0.62	0.37	0.73	0.59	0.17
Sericomyia silentis M	7	**0.97**	0.44	0.46	-0.08	-0.08	-0.60
Syrphus vitripennis	18	**0.95**	**0.76**	**0.75**	0.41	0.44	0.14
Volucella inanis	7	**1.00**	**0.86**	**0.85**	0.36	0.33	0.17

Table S6. MCMCglmm model of mimetic accuracy, which has been logit transformed. This model treats time of year as a continuous variable, as compared to Table 2 of the main article, in which season was treated as a two-level factor. For this purpose, "day" is a signed continuous variable calculated as the number of days before or after 8th August. We include a quadratic term for "day" to allow for a mid-season peak. SSU was included as a random effect, with a variance structure that accounts for phylogenetic relatedness. Backwards model selection was used on the basis of the pMCMC values. Posterior means are quoted for all predictors present in the minimum adequate model. All factors have df = 1. N = 638.

predictor	posterior mean	pMCMC
intercept	1.29	<0.001
proportion black	0.17	0.570
thorax width	0.083	0.206
sex (F)	0.46	<0.001
day	-0.0011	0.238
day^2		0.394
proportion black: thorax width	-0.22	0.020
proportion black: sex (F)	0.38	<0.001
thorax width: sex (F)	-0.19	<0.001
sex (F): day	0.0013	0.004
thorax width: day	0.0007	0.022
proportion black: day		0.114
sex (F): day^2		0.808
thorax width: day^2		0.752
proportion black: day^2		0.312

Table S7. MCMCglmm model of mimetic accuracy, which has been logit transformed. This model uses accuracy estimates based on all twelve model species, as compared to Table 2 of the main article, which uses data from the four most abundant models only. SSU was included as a random effect, with a variance structure that accounts for phylogenetic relatedness. Backwards model selection was used on the basis of the pMCMC values. Posterior means are quoted for all predictors present in the minimum adequate model. All factors have df = 1. N = 638.

predictor	posterior mean	pMCMC
intercept	1.25	0.006
proportion black	0.79	0.048
thorax width	0.14	0.098
sex (F)	0.60	<0.001
season (late)	-0.32	0.002
proportion black: thorax width	-0.29	0.032
proportion black: sex (F)	0.29	0.048
thorax width: sex (F)	-0.11	<0.001
sex (F): season (late)		0.550
thorax width: season (late)	0.047	0.012
proportion black: season (late)	0.33	0.024